An improved SVAT model calibration strategy based on the optimisation of surface temperature temporal dynamics

Benoît Coudert, Catherine Ottle

An improved SVAT model calibration strategy based on the optimisation of surface temperature temporal dynamics

B. Coudert[1] and C. Ottlé[1]

Received 14 November 2006; revised 19 January 2007; accepted 24 January 2007; published 28 February 2007.

[1] Various studies have demonstrated the potential of thermal infrared brightness temperature (TIR T_B) for monitoring surface exchanges of water and energy. This study focuses on the contribution of TIR T_B data for Land Surface Model (LSM) calibration. A numerical representation of the Soil-Vegetation-Atmosphere (SVA) transfers (SVAT model), named SEtHyS, was used. A calibration methodology of the model based uniquely on the optimisation of TIR T_B diurnal cycle features has been developed and applied, in an assimilation context, to the full vegetation period of a wheat crop. The results illustrate the advantages of such a methodology for the monitoring of environmental conditions simulated with the SVAT model, such as the root zone soil moisture. The impact of observation and simulation errors on TIR T_B was analysed and quantified in controlled numerical experiments. The results demonstrate the advantages of using relative temperature characteristics, instead of temperature values themselves, to minimise the impact of noise. **Citation:** Coudert, B., and C. Ottlé (2007), An improved SVAT model calibration strategy based on the optimisation of surface temperature temporal dynamics, *Geophys. Res. Lett.*, *34*, L04402, doi:10.1029/2006GL028778.

1. Introduction and Background

[2] SVAT (Soil Vegetation Atmosphere Transfers) models have been designed to compute both water and energy budgets at the SVA interface, with varying degrees of complexity in the described physical processes. These models allow the state variables, describing the transfer processes at different levels within the SVA continuum, to be assessed. They require an application context constrained by input variables (atmospheric forcing and vegetation variables) and input parameters (soil and vegetation properties, initialisation; see Table S1 of the auxiliary material)[1] to simulate the water and energy budget at the surface. The number of parameters is generally related to the complexity of the model, and their calibration requires the development of optimisation methodologies. Numerous studies of the characterisation of the surface properties and variables (soil moisture state, thermal inertia, soil texture) have been reported, based on the knowledge of surface temperature [*Price*, 1977; *Soer*, 1980; *Wetzel et al.*, 1984; *Wetzel and Woodward*, 1987; *Raffy and Becker*, 1985; *Raffy and Becker*, 1986; *Van de Griend et al.*, 1985; *Moran et al.*, 1994; *Carlson et al.*, 1995; *Xue and Cracknell*, 1995; *Cracknell and Xue*, 1996; *Sandholt et al.*, 2002; *Verhoef*, 2004; *Verstraeten et al.*, 2006]. The work described in the present paper concerns the application of a newly proposed methodology (B. Coudert et al., Monitoring land surface processes with thermal infrared data: Calibration of SVAT parameters based on the optimisation of diurnal surface temperature cycling features, submitted to *Remote Sensing of Environment*, 2007, hereinafter referred to as Coudert et al., submitted manuscript, 2007) used to control the simulated variables and input parameters of a Land Surface Model. The model used in this study, called SEtHyS (for "Suivi de l'Etat Hydrique des Sols", French acronym for soil moisture monitoring), is a two-layer, two-source SVAT model described by *Coudert et al.* [2006] based on *Deardorff*'s [1978] "force-restore" formalism for the soil representation. A model calibration based on the optimisation of temporal dynamics characteristics (temporal gradients, amplitude, phase) of the TIR (Thermal Infra Red) brightness surface temperature has been proposed by Coudert et al. (submitted manuscript, 2007), and applied over a seasonal winter wheat cycle at field scale. This method, in which time-differential temperature measurements are used, has been compared with a former method in which the absolute difference between modeled and observed temperature values are minimised at each time step (20 minute intervals) of the model (point-to-point optimization). The new method demonstrates distinct advantages, for the monitoring of SEtHyS SVAT output variables. The next step is to test this new methodology in a remote sensing brightness temperature automatic assimilation context, where both observations and model errors need to be handled. For this purpose, a dynamic calibration of the model was carried out. The impact of TIR T_B observational errors has also been quantified with a classical optimisation of the temperature method and the new methodology, and the results are presented in this paper. Section 2 briefly presents the calibration methodology and its objectives in an automatic assimilation context. Section 3 presents the application at field scale. Section 4 evaluates the sensitivity of this methodology to observation and model errors, and compares it with that obtained with classical optimisation of the TIR T_B variable.

2. Dynamic Calibration Methodology

[3] Previous studies [*Coudert et al.*, 2006, also submitted manuscript, 2007] showed the advantages of continuous recalibration of the SEtHyS SVAT model, in terms of

[1]Centre d'étude des Environnements Terrestre et Planétaires, Institut Pierre Simon Laplace, CNRS, Université de Versailles Saint-Quentin-en-Yvelines, Vélizy, France.

0094-8276/07/2006GL028778

[1]Auxiliary materials are available at ftp://ftp.agu.org/apend/gl/2006gl028778.

increased model performances. Depending on which time-dependent parameters are considered, and their sensitivity to the dominant transfer processes, surface conditions and atmospheric forcing, the use of regular optimisation procedures (which are then relevant to comparatively short calibration periods), has proven to be more accurate than a calibration methodology applied to the whole simulation period. Moreover, the use of TIR surface brightness temperature data in a multi-criteria model optimisation process where surface sensible heat flux, ground heat conduction flux, reflected solar incoming flux and soil water contents (surface and root zone) are adjusted, has demonstrated its potential for water budget monitoring [*Coudert et al.*, 2006]. Surface fluxes (sensible heat, latent heat, soil heat conduction fluxes), soil water content, atmospheric forcing and vegetation characteristics (Leaf Area Index and canopy height) measurements are in practice rarely measured simultaneously, and even then are limited to specific experimental field programmes, as was the case for the Alpilles-ReSeDA (Remote Sensing Data Assimilation) experiment [*Olioso et al.*, 2002] http://www.avignon.inra.fr/reseda/base/) briefly described below, whose database is used in the following. Conversely, thanks to the presence of space-borne remote sensing instruments, including new geostationary satellites which provide data with a high temporal frequency (around 15 mn), TIR T_B measurements are available, under clear sky conditions, at frequent intervals. Consequently, the development of a SVAT model calibration methodology, based on the knowledge of TIR T_B data, is of particular interest.

[4] The principle of our methodology computes the sensitivity of each model parameters to specific characteristics of the TIR T_B diurnal cycle, following the same statistical approach as *Bastidas et al.* [1999], and calibrates each model parameter by optimising a specific set of characteristics defined by the previous sensitivity analysis. The method differs from the multi-objective calibration proposed by *Gupta et al.* [1999] and *Demarty et al.* [2005], in that all the parameters are optimised with possible different sets of criteria (using the same set of simulations). In practice, just a specific set of criteria is used to calibrate each parameter, at each given time interval. This particular difference in approach is appropriate to the specific impact of the model parameters on the specific characteristics of the diurnal temperature cycle (morning rise, afternoon fall or amplitude, etc...). A previous application of this methodology (Coudert et al., submitted manuscript, 2007) concluded that, in addition to time-differential temperature criteria, a criterion related to the absolute difference between simulated and measured T_B would improve water budget monitoring, by limiting drifts in the computed value of root zone soil moisture.

[5] This improved calibration methodology has been applied to an automatic assimilation context, and the first results are presented in the present paper. In practice, instead of making use of successive a priori fixed model calibration periods, more exactly making model parameters readjustments (because the model parameters' uncertainty ranges are determined, for a given calibration period, by the results of the previous calibration), the model requiring recalibration is defined by the model errors on the brightness temperature. These model divergences are evaluated on the basis of the evolution of the set of TIR T_B criteria. The following section briefly presents the results obtained for a winter wheat crop field, recorded in the Alpilles-ReSeDA database.

3. Application at Field Scale

3.1. Alpilles-ReSeDA Database

[6] The Alpilles ReSeDA program was initiated to improve monitoring of soil and vegetation processes from remote sensing. A large database containing various types of data was recorded over the Alpilles (southeast of France) area from October 1996 to November 1997. Environmental conditions (agrometeorology, surface characteristics, multi-frequency remote sensing data and especially TIR data) were measured over various instrumented agricultural fields. In particular, ground based measurements of TIR T_B (8–14 micrometers) were acquired using a Heimann KT15 thermal radiometer 3 meters above the surface, with an 18.5° zenith angle and a 16° field of view. The dataset is quasi-complete and forms a continuous time series. Soil moisture profiles were measured with neutron (not regularly) and capacitive probes. The data was intercalibrated. Neutron probe data was used from 21st of January (DOY 21) and 19th of April (first rainfall episode, DOY 109) and capacitive probe data from 20th of April (DOY 110) to 25th of June (DOY 176). Latent and sensible heat fluxes were continuously measured (20′ time step) by means of both the Bowen ratio (over the whole period) and the Eddy correlation method (between 15th of March and 4th of April, DOY 74–94). The Bowen ratio deduced fluxes were reprocessed [*Olioso et al.*, 2002] because of over-estimations (bias of +15 $W.m^{-2}$) and a large scattering contribution (RMSD between 50 and 70 $W.m^{-2}$) compared with fluxes deduced using the correlation method. All these processes were carried out in order to obtain a coherent and continuous set of data corresponding to a complete vegetation cycle, for the validation and/or calibration of SVAT models [*Olioso et al.*, 2002].

3.2. Successive Readjustments

[7] The calibration process is driven by minimizing errors (as quantified by the Root Mean Square Difference, RMSD, over 20-day periods; see below) between the measured and modeled TIR T_B characteristics of the diurnal temperature cycle. More precisely, 7 of these criteria are related to *temporal gradients*, computed from the temperature rise and fall over 1 hour intervals in the morning and the afternoon (see the list of the criteria in Table S2 of the auxiliary material). Two additional criteria are given firstly by the *daily amplitude* of the temperature cycle, determined on the basis of the temperature maximum (around noon) and its value at sunset and secondly by the *phase* of the temperature signal, given by the time at which the daily maximum temperature is reached. The last criterion is not related to the diurnal temperature cycle characteristics but to the absolute difference between measured and modeled TIR T_B time series calculated over day-time (between sunrise and sunset). Notice that no RMSD are calculated for night-time values. The reason for this is that the parameterisation of atmospheric turbulence in SVAT models is not accurate in cases of strong stability which often occur during the

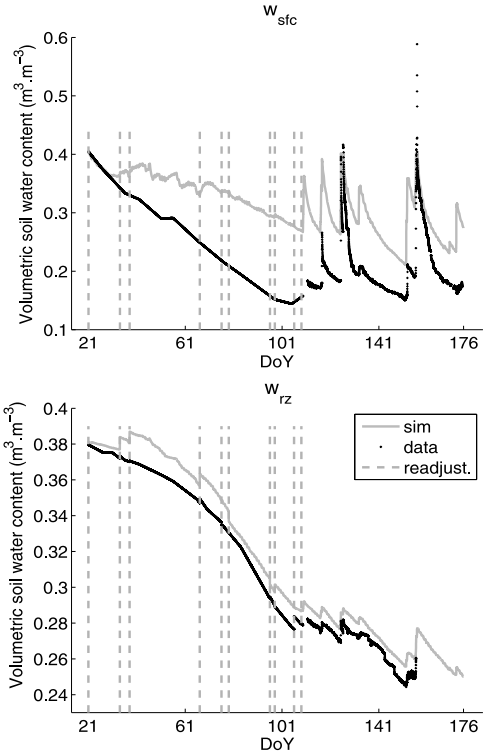

Figure 1. Soil water content time series obtained for the 10 calibration periods. The first day of each of the calibration periods is represented by grey, dashed vertical lines.

night. The resultantly greater model errors prevent the optimisation methodology from reaching correct solutions, especially for initial soil moisture states, as shown in previous studies (Coudert et al., submitted manuscript, 2007). Consequently, reduced uncertainty ranges (±2% of the simulated values) are determined at the first time step of a new calibration period, for re-initialisation of the soil water content (surface and root zone).

[8] The parameters' sensitivity-dependent calibration is carried out for 20-day periods, in order to compute the RMSD over a significant volume of data. Moreover 20-day periods are sufficiently short to provide adequate representation of the transitions between the vegetation's phases of growth, maturation and senescence, and of seasonal meteorological changes in our specific case of application. After each 20-day calibration period, the calibrated model parameters from that time interval are used to restart the model and to continue the model run beyond the calibration period. The accuracy of the prediction is evaluated using the Relative Root Mean Square Differences (RRMSD) which are normalised by dividing the differences between measured and modeled values by the measured values. The RRMSD are related to the 9 temperature features (*characteristics* of the diurnal temperature cycle) computed over a 20-day sliding temporal window, starting at the beginning of the calibration period. A new calibration is performed when one or several RRMSD increase by 50% with respect to the previous calibration period. Successive calibration periods can be intersected or disjoined, according to the evolution of the temperature features drifts.

3.3. Results

[9] Starting from the Day of Year (DoY) 21 (21st of January), 10 calibration periods were needed to monitor the SEtHyS simulations, using TIR T_B data assimilation, in order to reach DoY 129 (9th of May). No additional calibrations were carried out between the latter period of calibration (DoY 109 to 129) and the date at which the wheat was harvested (DoY 176, 25th of June) because the senesent phase had been reached and meteorological and surface conditions such as a soil drying phase or a rainfall event had all been encountered. Consequently, a new calibration was not expected to have a significant impact on model results for that particular time period. It is of interest to discuss the frequency of the calibration periods over the total period of simulation. All the calibration periods overlap with one another, except for the third (DoY 38–58) and the fourth (DoY 67–87), which are separated by 9 days. During this time interval (regular soil drying), atmospheric conditions were quite regular and the LAI was close to 1. The calibrated set of parameters obtained during the third period is thus accurate for a period of 29 days. For other periods, frequent readjustments are required because of variations in meteorological and phenological vegetation conditions, which affect the surface brightness temperature features.

[10] Figure 1 plots the results obtained for the surface water content (w_{sfc}) and the total root zone water content (w_{rz}, including the surface layer associated with w_{sfc}) time series, and includes a representation of the first day (readjustment) of each of the calibration periods. It can be seen that a very good degree of accuracy is obtained for the total water content w_{rz}, as opposed to that obtained for the surface soil water content simulation. The systematic overestimation of the latter variable can be explained by a tendency to overemphasise the soil's resistance to evaporation, which in turn leads to undervalued soil evaporation rates. The impact of this outcome on the simulations is particularly significant, since surface water content is high at the beginning of the simulation period and after intense rainfall events starting on DoY 109 (19th of April). A large shift (about 0.1 $m^3.m^{-3}$), compared to the observations, can then be observed. A similar result is observed when only TIR T_B is optimised. This additional criterion, used in the methodology presented here, thus appears to be responsible for the observed overestimation. On the other hand, after rainfall events, the soil drying rate is accurately estimated (DoY 117, 27th of April for example), thus showing that water diffusivity is accurately retrieved. The mean performances over the whole simulation period, between DoY 21 (21st of January) and DoY 176 (25th of June), are given in Table 1 in terms of biases and RMSD and also RRMSD and relative biases (relative to each measured value, as is the case for RRMSD, noted Rbiases). These statistical criteria are given for the following variables: TIR T_B, sensible heat flux (H), latent heat flux (LE), ground heat flux (G), net radiation (Rn) and solar reflected radiation (aR_g). Generally good results are obtained, with a mean RMSD of less than 45 $W.m^{-2}$ for the surface fluxes, and low biases (lower than 8 $W.m^{-2}$) with the exception of surface water content (w_{sfc}).

Table 1. Performances Obtained With the Calibration Methodology Over the Seasonal Wheat Cycle Between DoY 21 and 176

Variable	RMSD	Bias	*N* data
w_{sfc} ($m^3.m^{-3}$)	$9.5\ 10^{-2}$ RRMSD: 51.1%	$8.5\ 10^{-2}$ Rbias: 43.5%	10846
w_{rz} ($m^3.m^{-3}$)	$1.2\ 10^{-2}$ RRMSD: 3.8%	$1.1\ 10^{-2}$ Rbias: 3.6%	9582
LE ($W.m^{-2}$)	44.5	−4.1	3358
G ($W.m^{-2}$)	28.3	0.4	11055
H ($W.m^{-2}$)	43.4	−7.1	3358
aRg ($W.m^{-2}$)	24.4	12.7	5687
Rn ($W.m^{-2}$)	32.9	−12.8	11118
T_B (K)	1.78	−0.39	10903

This latter variable is overestimated by about 51% in terms of RRMSD, and by 44% in terms of Rbias.

[11] The relevance of the "readjustments" described here needs to be analysed, in order to ascertain the usefulness of the methodology in an assimilation context. To this intent, a comparison has been made between the soil water content simulations obtained from the first calibration period (DoY 21 to 41), and those obtained over the following calibration periods. Figure 2 shows, for both simulations, a plot of the RMSD calculated over a 20-day sliding window, from the first period up until DoY 176, which defines the end of the simulation period. This illustrates the cumulative effect of model errors, incurred by the dynamic calibration methodology. The model parameters calibrated on the first period would be inappropriate, particularly after DoY 121. In the case of this application, these results illustrate the interest of successive readjustments in controlling the cumulated error of the model related to soil water contents.

[12] The following section is devoted to the study of the influence of TIR T_B estimation errors on calibration results, in the case of a controlled simulation. A detailed comparison is given for a simple calibration, based on point-to-point (at the model time step) TIR T_B optimisation.

4. Impact of Errors

4.1. Sources of Error

[13] Differences between modeled and measured TIR T_B time series result from both observational and model errors. In the case of our application, *observational errors* are the smallest. The ground-based Heimann KT15 thermal radiometer, used to measure surface brightness temperature, is characterised by a minimum error of 0.7 K (A. Olioso, personal communication, 2006). Since its commissioning, this sensor has demonstrated negligible drift over a one year period of experimental recordings. When space-borne remote sensing data is used, observational errors would include additional atmospheric and surface emissivity correction errors, as well as various other sources of error such as registration uncertainties and calibration effects resulting from the presence of clouds. *Simulation errors* arise from *model input errors* (atmospheric forcing, vegetation input variables) and from *model simulation errors* (incorrect representation of physical processes). Although the former effects can have a strong impact on the simulation results, their discussion is beyond the scope of this paper. The latter forms of error are responsible for systematic biases and characteristic features of computed TIR T_B. This has been illustrated by *Coudert et al.* [2006] and *Olioso et al.* [1996] who showed, for example, the impact on surface fluxes and TIR T_B simulations of a simplified stomatal resistance representation in SVAT models.

[14] In order to evaluate the impact of such errors on the calibration methodology, a set of controlled numerical calibration experiments has been carried out in the presence of various levels of noise. The results of these experiments are presented in the following.

4.2. Application in a Simulated Case

[15] A SVAT simulation performed with a calibrated parameter set resulting from a multi-objective calibration on the same Alpilles-ReSeDA experimental dataset, was used as a reference. The 6 criteria simultaneously optimized (referred to as *scenario 1* in *Coudert et al.* [2006]) are related to the surface fluxes, TIR T_B and the soil water contents. This scenario controls all terms of the water and

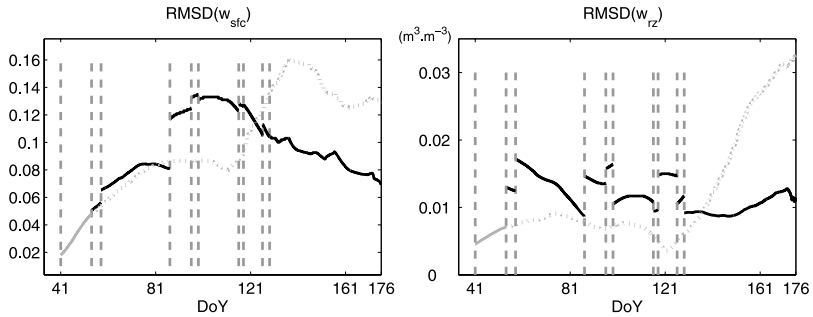

Figure 2. Soil water contents RMSD calculated for a 20 day sliding window. Simulations obtained from the first calibration period (DoY 21–41) are in grey. Simulations from successive readjustments are in black. DoY indicated on the x axis are the final days of the calibration periods.

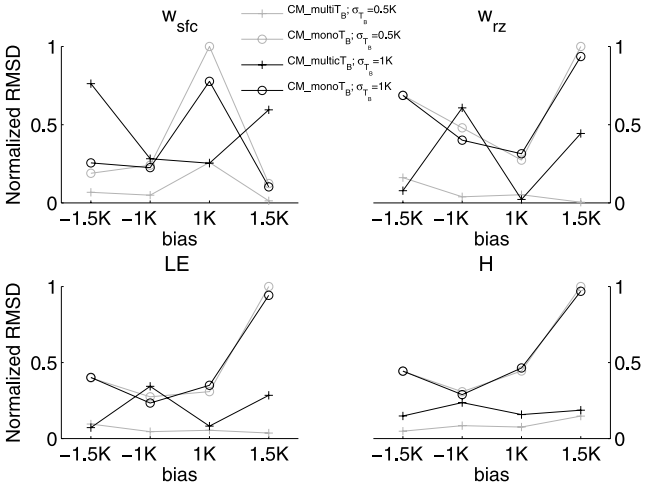

Figure 3. Normalised RMSD obtained for both calibration methodologies, CM_multiTB and CM_monoTB, for each of the experiments characterised by the 8 different permutations of the two noise parameters (m_{TB}, σ_{TB}).

energy budget and the resulting calibrated parameters were used to produce a reference model run. The modeled surface brightness temperature time series obtained from this run was used instead of observations. This synthetic set of observations was useful to study the impact of observational errors on the calibration process, because they could be statistically controlled. The synthetic TIR T_B time series data, over the period DoY 74–94 (wheat growing period with regular soil drying), was degraded by the addition of noise in terms of biases and random errors. The errors were assumed to be Gaussian with a standard deviation σ_{T_B} (0.5 K, 1 K), and the biases were taken as m_{T_B} (−1.5 K, −1 K, 1 K, 1.5 K). The impacts of such errors have been evaluated on both calibration methodologies: the calibration proposed in this paper based on the TIR T_B diurnal cycle characteristics (referred to in the following as *CM_multiT_B*), and the former (classical) calibration based on the simple optimisation of point-to-point TIR T_B values (referred to as *CM_monoT_B*). Each of the above two model calibrations was then performed for each of the experiments characterised by the 8 different permutations of the two noise parameters (m_{T_B}, σ_{T_B}). The results obtained from both methodologies are shown in Figure 3, for surface fluxes *LE* and *H* and for soil water contents (w_{sfc} and w_{rz}).

[16] RMSD values obtained with a given calibration methodology and a given value of σ_{T_B} are linked by the same line. For each variable, the RMSD obtained with a given experiment is normalized by the minimum (0 in Figure 3) and the maximum (1 in Figure 3) RMSD values obtained from the 16 calibrations achieved. It can be seen that *CM_multiT_B* gives better results than *CM_monoT_B* for σ_{T_B} = 0.5 K (low temperature noise) whatever the value of the bias. When the value of σ_{T_B} increases (σ_{T_B} = 1 K), *CM_multiT_B* conserves its advantage (excepted for w_{sfc}) for the larger biases (−1.5 K and 1.5 K) but is more sensitive to random errors than *CM_monoT_B*. It is interesting to note that the two cases σ_{T_B} = 0.5 K and σ_{T_B} = 1 K lead to almost identical results for *CM_monoT_B* (the black and grey lines are nearly identical) as opposed to the *CM_multiT_B* method. Note that maximum RMSD on LE and H are respectively 85 and 74 W.m^{-2} when *CM_monoT_B* is used, to be compared with respectively 25 and 15 W.m^{-2} when *CM_multiT_B* is used, for m_{T_B} = 1.5 K. The results obtained for w_{sfc} with *CM_monoT_B* are surprising, when m_{T_B} = 1 K because the largest RMSD were expected for the largest absolute values of m_{T_B}. In fact, the largest RMSD are obtained for m_{T_B} = 1 K and the RMSD on variables aRg and Rn show the same features (not presented here). The solution of the calibration reached by *CM_monoT_B* for this value of m_{T_B} is the following: the surface albedo is minimal (over the prescribed parameter uncertainty range) and the saturated hydraulic conductivity parameter converges towards the upper limit of its uncertainty range. Such a combination is not accurate for simulations of aRg, Rn and w_{sfc}, and is not in general the solution obtained by the calibration for other bias values but leads to a better solution for the optimization of TIR T_B. Table 2 shows the RMSD dispersion with the bias m_{T_B} for the SEtHyS output variables. More precisely, this dispersion is the difference between the maximal and minimal values of normalized RMSD for the same σ_{T_B} (each line of the plots in Figure 3) compared to 1 (the result is a percentage). An expected result is the low sensitivity of *CM_multiT_B* to bias, since the random error on TIR T_B is low. The dispersion is lower than 30% for the complete set of variables, whereas *CM_monoT_B* has a dispersion ranging between 60 and 90 %. Since σ_{T_B} increases up to 1 K, the dispersion on RMSD due to the bias is still lower for *CM_multiT_B* than *CM_monoT_B*, except for aR_g and consequently R_n. In practice, aR_g depends only on the albedo, the calibration of which can be strongly affected by random errors, especially with the *CM_multiT_B* method,

Table 2. Percentage Dispersion of RMSD Obtained by Application of 4 Different Values of Bias for Both Calibration Methodologies[a]

	σ_{TB}, 0.5 K		σ_{TB}, 1 K	
Variable	CM_monoT$_B$, %	CM_multiT$_B$, %	CM_monoT$_B$, %	CM_multiT$_B$, %
w_{sfc}, M^3.m^{-3}	87.6	24.5	67.4	50.9
w_{rz}, m^3.m^{-3}	72.7	15.8	62.1	58.6
LE, W.m^{-2}	72.6	5.9	70.8	27.2
G, W.m^{-2}	61.8	11.0	53.9	46.4
H, W.m^{-2}	69.3	9.9	68.0	8.8
aRg, W.m^{-2}	67.6	23.0	32.9	45.4
Rn, W.m^{-2}	70.1	25.8	39.2	60.7
T_B, K	10.6	27.9	3.4	45.9

[a]Bias is m_{T_B}.

because of the greater sensitivity of TIR T_B characteristics to noise, when compared to the point-to-point complete cycle optimisation for which the effect of the noise is averaged.

5. Conclusions

[17] A dynamic calibration methodology based on the SEtHyS SVAT model parameters' sensitivities to the diurnal surface TIR T_B features has been proposed in an assimilation context. Correct root zone soil moisture monitoring is obtained in this applied case, over the full seasonal cycle of a wheat crop. However, surface soil moisture is overestimated due to poor retrieval of the soil's resistance to evaporation. A set of ten 20-day calibration periods was needed to control the SVAT model over more than 100 days of simulation. Compared with a calibration based on a simple optimisation of TIR T_B simulations with respect to measured values, the proposed methodology shows better results and a lower sensitivity to error biases on T_B, but becomes unstable when the random errors increase. This work demonstrates that TIR T_B diurnal variations contain useful information for SVAT model monitoring, but that further development are needed in order to develop operational techniques for assimilating thermal infrared data into SVAT models. The use of time-differential criteria on remotely sensed surface temperatures has been shown to be promising in terms of recent and future high temporal data-rate acquisitions, in preventing observational error biases from degrading the assimilation results.

[18] The stochastic calibration technique presented in this paper has the advantage of being straightforward to implement, although it requires considerable computing resources and is necessarily limited to optimisation problems with a relatively small number of degrees of freedom.

[19] The next step in this study programme will involve the further development of operational assimilation techniques, in order to test the usefulness of rapid refresh rate remote sensing satellites, such as Meteosat-8 and 9, to control water and energy budgets over regional landscapes, with the spatial resolution of the SVAT model.

[20] **Acknowledgments.** The work described here was funded by the French national programme, INSU-PNTS. The authors wish to thank the French Space Agencies, CNES and ONERA, for the scholarship support they provided for this study. Particular thanks are extended to all the participants of the Alpilles-ReSeDA experiment for making their database available. The authors are also grateful to A. Olioso, J. Demarty and X. Briottet for numerous constructive discussions, and to anonymous reviewers for their careful reading and useful suggestions to improve the manuscript.

References

Bastidas, L. A., H. V. Gupta, S. Sorooshian, W. J. Shuttleworth, and Z. L. Yang (1999), Sensitivity analysis of a land surface scheme using multicriteria methods, *J. Geophys. Res.*, *104*, 19,481–19,490.

Carlson, T. N., R. R. Gillies, and T. G. Schmugge (1995), An interpretation of methodologies for indirect measurement of soil water content, *Agric. For. Meteorol.*, *77*, 191–205.

Coudert, B., C. Ottlé, B. Boudevillain, J. Demarty, and P. Guillevic (2006), Contribution of thermal infrared remote sensing data in multiobjective calibration of a dual source SVAT model, *J. Hydrometeorol.*, *7*, 404–420.

Cracknell, A. P., and Y. Xue (1996), Thermal inertia determination from space—A tutorial review, *Int. J. Remote Sens.*, *17*, 431–461.

Deardorff, J. W. (1978), Efficient prediction of ground surface temperature and moisture, with inclusion of a layer of vegetation, *J. Geophys. Res.*, *83*, 1889–1903.

Demarty, J., C. Ottlé, I. Braud, A. Olioso, J. P. Frangi, H. V. Gupta, and L. A. Bastidas (2005), Constraining a physically based soil-vegetation-atmosphere transfer model with surface water content and thermal infrared brightness temperature measurements using a multi-objective approach, *Water Resour. Res.*, *41*, W01011, doi:10.1029/2004WR003695.

Gupta, H. V., L. A. Bastidas, S. Sorooshian, W. J. Shuttleworth, and Z. L. Yang (1999), Parameter estimation of a land surface scheme using multi-criteria methods, *J. Geophys. Res.*, *104*, 19,491–19,503.

Moran, M. S., T. R. Clarke, Y. Inoue, and A. Vidal (1994), Estimating crop water deficit using the relation between surface-air temperature and spectral vegetation index, *Remote Sens. Environ.*, *49*, 246–263.

Olioso, A., T. N. Carlson, and N. Brisson (1996), Simulation of diurnal transpiration and photosynthesis of a water stressed soybean crop, *Agric. For. Meteorol.*, *81*, 41–59.

Olioso, A., et al. (2002), Monitoring energy and mass transfers during the Alpilles-ReSeDA experiment, *Agronomie*, *22*, 597–610.

Price, J. C. (1977), Thermal inertia mapping: A new view of the Earth, *J. Geophys. Res.*, *82*, 2582–2590.

Raffy, M., and F. Becker (1985), An inverse problem occurring in remote sensing in the thermal infrared bands and its solutions, *J. Geophys. Res.*, *90*, 5809–5819.

Raffy, M., and F. Becker (1986), A stable iterative procedure to obtain soil surface parameters and fluxes from satellite data, *IEEE Trans. Geosci. Remote Sens.*, *GE-24*, 327–333.

Sandholt, I., K. Rasmussen, and J. Andersen (2002), A simple interpretation of the surface temperature/vegetation index space for assessment of surface moisture status, *Remote Sens. Environ.*, *79*, 213–224.

Soer, G. J. R. (1980), Estimation of regional evapotranspiration and soil moisture conditions using remotely sensed crop surface temperature, *Remote Sens. Environ.*, *9*, 27–45.

Van de Griend, A. A., P. J. Camillo, and R. J. Gurney (1985), Discrimination of soil physical parameters, thermal inertia and soil moisture from diurnal temperature fluctuations, *Water Resour. Res.*, *21*, 997–1009.

Verhoef, A. (2004), Remote estimation of thermal inertia and soil heat flux for bare soil, *Agric. For. Meteorol.*, *123*, 221–236.

Verstraeten, W. W., F. Veroustraete, C. J. van der Sande, I. Grootaers, and J. Feyen (2006), Soil moisture retrieval using thermal inertia, determined with visible and thermal spaceborne data, validated for European forests, *Remote Sens. Environ.*, *101*, 299–314.

Wetzel, P. J., and R. H. Woodward (1987), Soil moisture estimation using GOES-VISSR infrared data: A case study with a simple statistical method, *J. Clim. Appl. Meteorol.*, *26*, 107–117.

Wetzel, P. J., D. Atlas, and R. H. Woodward (1984), Determining soil moisture from geosynchronous satellite infrared data: A feasibility study, *J. Clim. Appl. Meteorol.*, *23*, 375–391.

Xue, Y., and A. P. Cracknell (1995), Advanced thermal inertia modelling, *Int. J. Remote Sens.*, *16*, 431–446.

B. Coudert and C. Ottlé, Centre d'étude des Environnements Terrestre et Planétaires, Institut Pierre Simon Laplace, CNRS, Université de Versailles Saint-Quentin-en-Yvelines, 10–12, avenue de l'Europe, F-78340 Vélizy, France. (benoit.coudert@cetp.ipsl.fr)